LIQUEFACTION MODEL CONSIDERING SOLID TO FLUID TRANSITION BASED ON INTERNAL EROSION

J. Kurima[(1)], Y. Shingaki[(2)], H. Goto[(3)], S. Sawada[(4)]

[(1)] *Graduate Student, Graduate School of Engineering, Kyoto University, kurima@catfish.dpri.kyoto-u.ac.jp*
[(2)] *Researcher, Tokyo Electric Power Services Co., Ltd., shingaki@tepsco.co.jp*
[(3)] *Associate Professor, Disaster Prevention Research Institute, Kyoto University, goto@catfish.dpri.kyoto-u.ac.jp*
[(4)] *Professor, Disaster Prevention Research Institute, Kyoto University, sawada@catfish.dpri.kyoto-u.ac.jp*

Abstract

In order to predict damages due to soil liquefaction, it is important to estimate not only the location where the liquefaction is likely to occur, but also the amount of deformation after the occurrence. The soil ground behaves as a solid until the liquefaction, while it behaves as a fluid during the liquefaction. Understanding of a physical process of solid to fluid transition of the soil ground is a key factor to estimate the amount of deformation precisely.

We assume two essential process of solid to fluid transition; 1) soil particles are constrained in the vicinity of the soil skeleton while reducing the number of particle contacts, and 2) the particles float and flow together with the pore water. The processes correspond to increase of the pore water pressure and the shear strain, respectively. In fact, laboratory experiments have shown that the time evolution of pore water pressure prior to the evolution of shear strain. The conventional dilatancy model cannot explain the lag of evolution, and therefore, cumulative plastic strain has been a popular parameter to represent this nature.

In this study, we introduce an internal erosion instead of the cumulative plastic strain during the liquefaction. Three-phase model of saturated soil proposed by Fujisawa et al. (2010), which include a new phase of eroded particles, is applied to our model, and the conservation of momentum is newly derived. The model is compared with the conventional constitutive model through the results of laboratory tests, and is validated by comparing the results of shaking table tests in the centrifuge.

The proposed liquefaction model reproduced a progress of stiffness degradation even after the excess pore pressure increased sufficiently without parameters related to the cumulative plastic strain. The internal erosion acts to extract particles from the soil skeleton. As a result, the porosity increases and the behavior becomes looser sand. From the the shaking table test, the acceleration, excess pore pressure and shear stiffness degradation are well simulated in comparison to the observed ones. This suggests that the model can represent the principal feature of liquefaction.

Keywords: liquefaction, internal erosion, three-phase model of saturated soil

1. Introduction

The liquefaction behavior has been investigated through laboratory tests, i.e., triaxial cyclic loading tests. When liquefaction occurs, excess pore water pressure increases and reaches initial effective confining pressure. After the progress, shear strain starts to accumulate and then the soil behaves like a fluid, e.g., lateral spreading, etc. In the numerical analysis, if the stiffness depends on the effective confining pressure, it is impossible to reproduce the increase of shear strain after the effective confining pressure reaches zero, so the degradation of stiffness is expressed using the accumulated plastic strain as a parameter. However, it is not fully understood the physical reason why stiffness degradation is delayed from the increase of excess pore water pressure.

We assume two essential processes of solid to fluid transition during the liquefaction; 1) soil particles are constrained in the vicinity of the soil skeleton while reducing the number of particle contacts, and 2) the particles float and flow together with the pore water. Under the cyclic loadings, the pore water pressure increases and then saturates, which correspond to the first process. At this time, the strain is not well developed. Applying more cyclic loadings, the deformation gradually increases, which correspond to the second process.

In this study, we introduce an internal erosion during the liquefaction as the mechanical process, which aims to represent degradation of stiffness by the transition of the soil ground. Fujisawa et al. (2010) proposed a three-phase model by introducing a new phase of eroded particles into the conventional two-phase model for saturated soil. Eroded particle is floating and flow with pore water. The internal erosion is represented as a process of phase transfer from soil skeleton to the eroded particles. We examine to adopt the three-phase model to represent the liquefaction process, and it is validated with the experimental results.

In order to introduce the three-phase model into the liquefaction analysis, a conservation of momentum is required in addition to the conservation of mass, which was formulated by Fujisawa et al. (2010). In this paper, we first derive the governing equations for the three-phase model, including the conservation of momentum. The model is compared with the conventional constitutive model through the results of laboratory tests, and it is shown that the process of degradation of stiffness is able to be represented without using the cumulative strain. Then, the model is validated by comparing the results of shaking table tests in the centrifuge.

2. Governing Equation of Three-phase Model for Saturated Soil

2.1. Three-phase model for saturated soil

In this study, we adopt the three-phase model of saturated soils proposed by Fujisawa et al. (2010). Figure 1 shows concepts of the conventional two-phase model and the three-phase model. The three-phase model includes an additional phase consisting of the eroded particles, which represent the particle floatation from the soil skeleton. Pore liquid is defined by the sum of phases of pore water and eroded particles. The physical quantities of the three-phase model are defined as follows.

$$n_{III} \equiv 1 - \frac{V_{ss}}{V},\ C \equiv \frac{V_{sw}}{V_l}\ \left(V \equiv V_l + V_{ss}\right), \tag{1}$$

where V and Vss are volumes of the total soil mass and soil skeleton, respectively. Vsw is a volume of eroded particles, which are assumed to float in the pore water. V_l is a volume of a pore liquid defined by the sum of the eroded particles and the pore water. n_{III} is a porosity of the three-phase model. C is a concentration of the eroded particles in the pore liquid. Density of the pore liquid ρ_f is represented, as follows.

$$\rho_f = \frac{V_{sw}}{V_l}\rho_s + \left(1 - \frac{V_{sw}}{V_l}\right)\rho_w = C\rho_s + \left(1 - C\right)\rho_w, \tag{2}$$

where ρ_s and ρ_w are densities of the soil particles and pore water, respectively. Mass of each phase per unit volume is expressed, as follows.

$$\overline{\rho_s} = \frac{V_{SS}}{V}\rho_s = (1 - n_{\mathrm{III}})\rho_s \,, \tag{3}$$

$$\overline{\rho_e} = \frac{V_{SW}}{V}\rho_s = C n_{\mathrm{III}}\rho_s \,, \tag{4}$$

$$\overline{\rho_f} = 1 - \frac{V_{SS}}{V}\rho_f = n_{\mathrm{III}}\rho_f \,, \tag{5}$$

where $\overline{\rho_s}$, $\overline{\rho_e}$, and $\overline{\rho_f}$ are for the soil skeleton, eroded particles, and pore liquid, respectively.

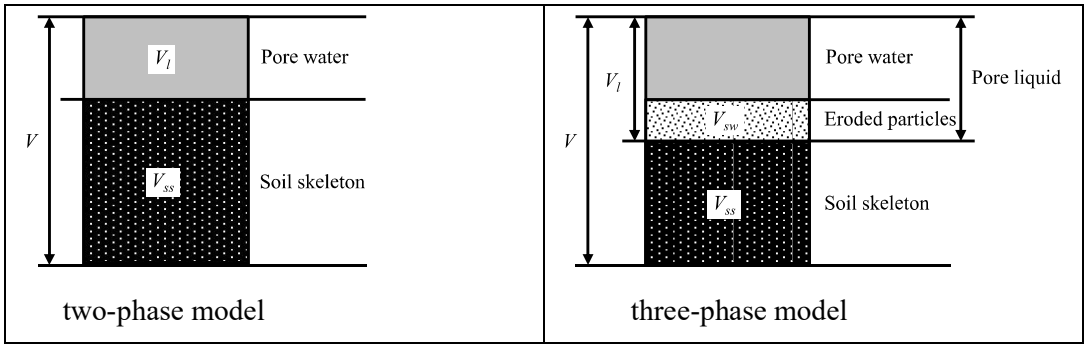

Figure 1. Concept of two-phase model (conventional model) and three-phase model (Fujisawa et al., 2010) for saturated soil.

2.2. Governing equation

Governing equations for the three-phase model are derived under the assumption that the eroded particles move together with the pore water. In this study, we omit the deposition and advection processes.

Eq.(6) and Eq.(7) are the equation of motions for the soil skeleton and for the pore liquid, respectively.

$$(\rho - \overline{\rho_f})\ddot{u}_i + \dot{n}_{III}\rho_f(\dot{U}_i - \dot{u}_i) - n_{III}\dot{\rho}_f\dot{u}_i + \sigma'_{ij,j} + (1 - n_{III})p_{,i} - \frac{\rho_f g}{k}n_{III}^2(\dot{U}_i - \dot{u}_i) - (\rho - \overline{\rho_f})b_i = 0 \tag{6}$$

$$\rho_f\ddot{U}_i + \dot{\rho}_f\dot{U}_i = -p_{,i} - \frac{\rho_f g}{k}n_{III}(\dot{U}_i - \dot{u}_i) + \rho_f b_i, \tag{7}$$

where p and σ'_{ij} are an excess pore water pressure and an effective stress tensor, respectively. k is a hydraulic conductivity, which is defined as permeability of pore liquid flow to the soil skeleton. g is the gravity acceleration. The second term on the right side of Eq.(7) indicates an interaction term between the pore liquid and the soil skeleton shown in Nishimura (1999).

Compared to the conventional equations, terms corresponding to the porosity and density changes are added.

2.3. Erosion rate

The internal erosion process is formulated by erosion rate, which controls a particle transport from the soil skeleton to the eroded particles. The erosion rate is assumed to be a function of hydraulic shear stress τ_f, which is the frictional stress caused by local micro-seepage flows. Previous studies based on experimental results and semi-theoretical derivations have proposed the following erosion rate model(e.g., Indraratna et al., (2009)).

$$E = \alpha\langle\tau_f - \tau_c\rangle \,, \tag{8}$$

where α is an erodibility coefficient, and τ_c is a critical shear stress. Bracket ⟨ ⟩ indicates McCauley brackets, ensuring the erosion does not occur when $\tau_f < \tau_c$.

With the erosion rate, increment of porosity is defined as followed by Fujisawa et al. (2010).

$$\frac{\partial n_{III}}{\partial t} = EA_e \,, \tag{9}$$

where A_e is the surface area of the erodible region per unit volume.

2.4. Hydraulic shear stress

Here, we assume that local micro-seepage flows of pore liquid generate the hydraulic shear stress. The micro-seepage flow in any of the void space of the soil skeleton is assumed to be approximated by a one-dimensional cylindrical flow, Hagen-Poiseuille flow. The hydraulic shear stress acting on the tube wall τ_f can be represented as follows.

$$\tau_f = C_{HP}\frac{e_{III}^2}{1+u_{i,i}}p,\ C_{HP} = \frac{4}{3}\pi\frac{C_T D^3}{(1-n_{III0})V_0}. \tag{10}$$

where C_{HP} is the dimensionless constant parameter, and C_T is the material constant corresponding to the shape factor. V_0 and n_{III0} are the initial values

3. Numerical test 1 – cyclic torsional shear test

The test is the undrained shear torsion test of Toyoura sand (Uemura, (2010)). Particle size is ranged in 0.075–0.850mm, and uniformity coefficient is 1.635. Specific gravity is 2.659, maximum void ratio is 0.991, and minimum void ratio is 0.624. Relative density of the test sample is 30.9%. The maximum value of the shear loading relative to the initial effective confining pressure (98 kPa) is 0.20. The cyclic load is the sine function with a frequency of 0.1 Hz.

An elasto-plastic model by Li (2002) is adopted to the numerical simulations. The model represents the behavior of sand as a function of state parameter ψ, which depends on the effective confining pressure and porosity. Increase of the shear strain after saturating the pore water pressure is controlled by a function f_L, which is a function of the cumulative plastic strain deviation. We adopt the proposed internal erosion model instead of the f_L.

We compare the results of three models. The first one (conventional model I) is the conventional elasto-plastic model by Li (2002), containing the original definition of f_L. The second one (conventional model II) is a conventional model excluding the contribution of f_L. The model is expected to show no increases of shear strain after saturating the pore water pressure. The final one is the proposed model, which incorporates the internal erosion model instead of the contribution of f_L.

Figure 2 shows the results of laboratory experiment and numerical simulations. 5 cyclic loadings are applied for the experiment and the simulations, but for the conventional model II, 20 cyclic loadings are applied. The experimental result shows clear increase of the shear strain after the excess pore water pressure reaches 95% (dotted line) of the initial effective confining pressure. The numerical result of the conventional model I well represents evolution of the shear strain, while the conventional model II cannot explain the evolution. This suggests that the shear strain increase is controlled by a function of cumulative plastic strain in the conventional model. The proposed model can represent the shear strain evolution well without using the cumulative parameters. In the laboratory test, an inverse S-shaped hysteresis is shown in the relation between the shear strain and shear stress. The conventional model I represent the shapes well. On the other hand, the proposed model cannot represent the hardening.

Figure 3 shows change of void ratio and change of equivalent shear stiffness per cyclic loading by the proposed model. The increase in porosity is caused by the internal erosion, floatation of soil particles from the soil skeleton. The degradation of stiffness is controlled by the change of porosity, which governs the deformation behavior of the soil skeleton through the state parameter ψ. With increasing the porosity, the behavior changes to looser sand. As a result, the shear stiffness decreases,

and the shear strain increases. The proposed model represents the physical process of solid to fluid transition through the change of porosity.

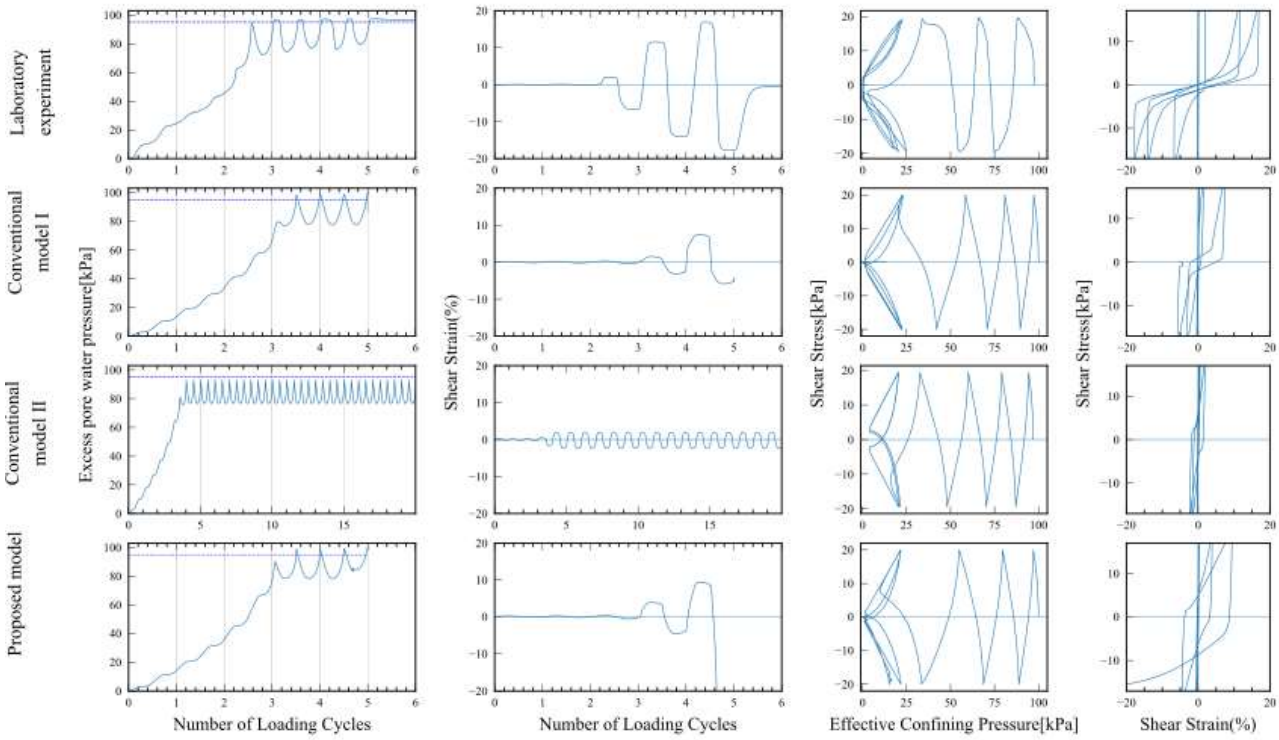

Figure 2. Numerical results of cyclic torsional shear test. Comparison of number of loading cycles versus shear strain, number of loading cycles versus shear stress, effective stress path, and shear stress versus shear strain.

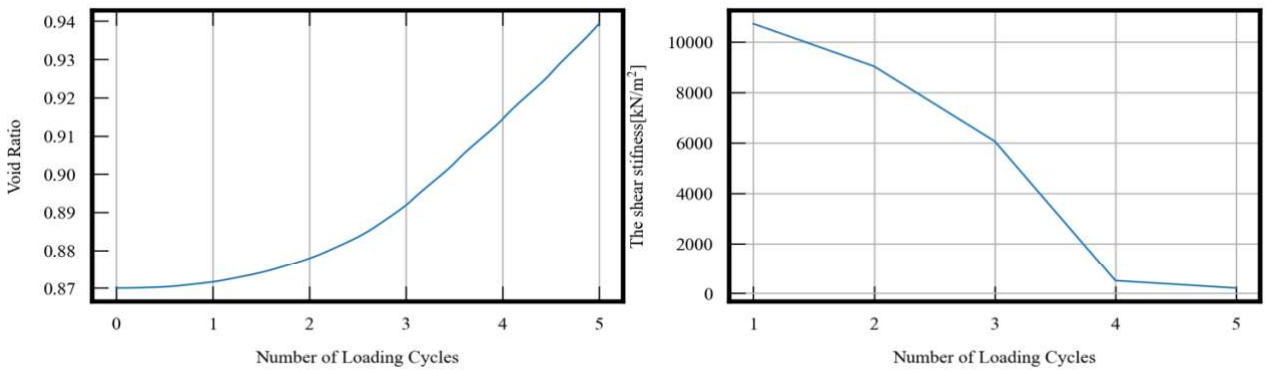

Figure 3. Evolution of void ratio and degradation process of equivalent shear stiffness

4. Numerical test 2 – centrifuge test

The proposed model is adopted to simulate the centrifugal test by Watanabe et al.(2018), which was aimed to measure changes in permeability during liquefaction. The model ground consists of homogeneous saturated Toyoura sand, as shown in Figure 4. The specific gravity is 2.669, maximum void ratio is 0.99, and minimum void ratio is 0.640. The permeability is 0.023cm/s when the void ratio and relative density are 0.76 and 63.4%, respectively. The bottom surface at a depth of 5m in prototype dimension is an impermeable boundary. The density and viscosity of the pore water are adjusted so that it becomes equivalent to water under the given gravity field of 25G. Input wave of the test is shown in Figure 5.

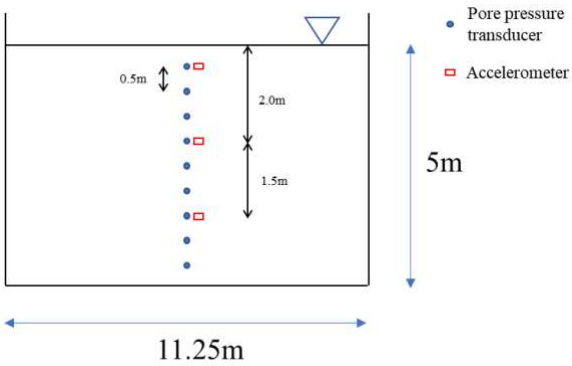

Figure 4. Proto type model of the centrifuge test by Watanebe et al.(2018)

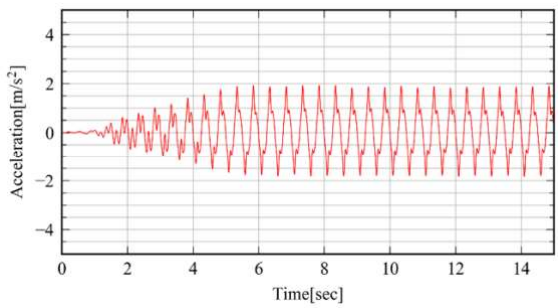

Figure 5. Input acceleration of the centrifuge test by Watanebe et al.(2018)

The numerical model is shown in Figure 6. Height of the soil ground is 5m. The domain is divided into 0.5m width elements. Right and left sides of the domain are set to be cyclic boundaries. Bottom of the domain is assumed to be a rigid basement. We set all nodes to undrain condition ($u_i = U_i$). The specific gravity, maximum void ratio, minimum void ratio, water density, viscosity, and permeability are the same values as the centrifuge test. The other parameters are gravitational acceleration 9.8m/s^2 and size of sand particle 0.172mm.

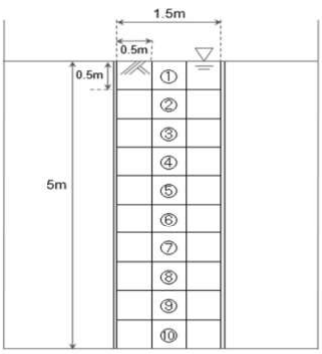

Figure 6. Numerical model for the centrifuge test.

In the proposed model, the porosity increases with progress of internal erosion, and this causes instability when the porosity becomes very large. To prevent this, upper bound of the void ratio e_{lim} is introduced, and the erosion is terminated after reaching the value. We consider that internal erosion is most rapid in the early stages, and slow as it approaches liquefaction. The erosion rate is modified by the following logarithm function.

$$\frac{\partial n_{III}}{\partial t} = EA_e \cdot \{-\log\left(1 - \frac{e_{lim}-e}{e_{lim}-e_0}\right)\} \tag{11}$$

where e_0 is the initial void ratio.

Figure 7 compares time evolutions of the excess pore water pressure and acceleration obtained from the experiment and the proposed model. The proposed model simulates the experimental results of excess pore water pressure well. However, it shows that the result of excess pore water pressure at the layers close to the surface is not well accurate especially for 0.5 m. This suggests that when the initial effective confining pressure is small, the results tend to be not well simulated. The result of acceleration is more accurate in the bottom layer as well as that of excess pore water pressure. The results at 2.0 m are well simulated until about 6.0 seconds, however, similar results for 0.5 m, the following process that increases the acceleration amplitudes and their reduction cannot be simulated by proposed model.

Figure 8 shows the shear strain and the shear stress relationship and the effective stress path at 2.0 m and 3.5 m. The proposed model simulates the stiffness reduction well. On the other hand, the shear stress is never completely zero during liquefaction. Because of the void ratio limitation e_{lim} for numerical stability, the shear stress does not reach zero and the degradation of stiffness is not sufficiently reproduced after liquefaction. It is considered that this inhibits representing the process of the acceleration amplitude reduction after 7.5 seconds. From the effective stress path, the effective confining pressure reaches almost zero. However, it does not show a large recovery of effective confining pressure. To represent a large effective confining pressure by considering both erosion and deposition processes is important to describe the behavior during liquefaction under cyclic loading and will be addressed as a future work.

5. Discussion and Conclusion

In this article, we propose internal erosion is introduced in the liquefaction analysis. We explain the erosion rate of soil based on the micro-seepage flow, and the governing equations, including the conservation of momentum for the three-phase model which was proposed by Fujisawa et al. (2010).

The numerical simulation of cyclic loading tests shows the proposed model can reproduce degradation of stiffness is delayed from excess pore water pressure reaching initial effective confining pressure without using cumulative plastic strain. The numerical result also shows the increase in the void ratio due to internal erosion changes the behavior of the sand to that of loose sand.

The results of the centrifuge test show that the proposed model can reproduce the excess pore water pressure and acceleration well, excepting the results near the free surface. On the other hand, upper bound of the void ratio is set for stability of the analysis, therefore, the degradation of stiffness is not sufficiently and the shear stress do not reach zero completely.

6.Acknowledgment

We would like to show our greatest appreciation to Professor Koji Ichii at Kansai University and Kazuaki Uemura at OYO Corporation for providing the data set of undrained torsional shear test conducted at Hiroshima University. We used a part of the data in order to perform the numerical simulation of a liquefaction test.

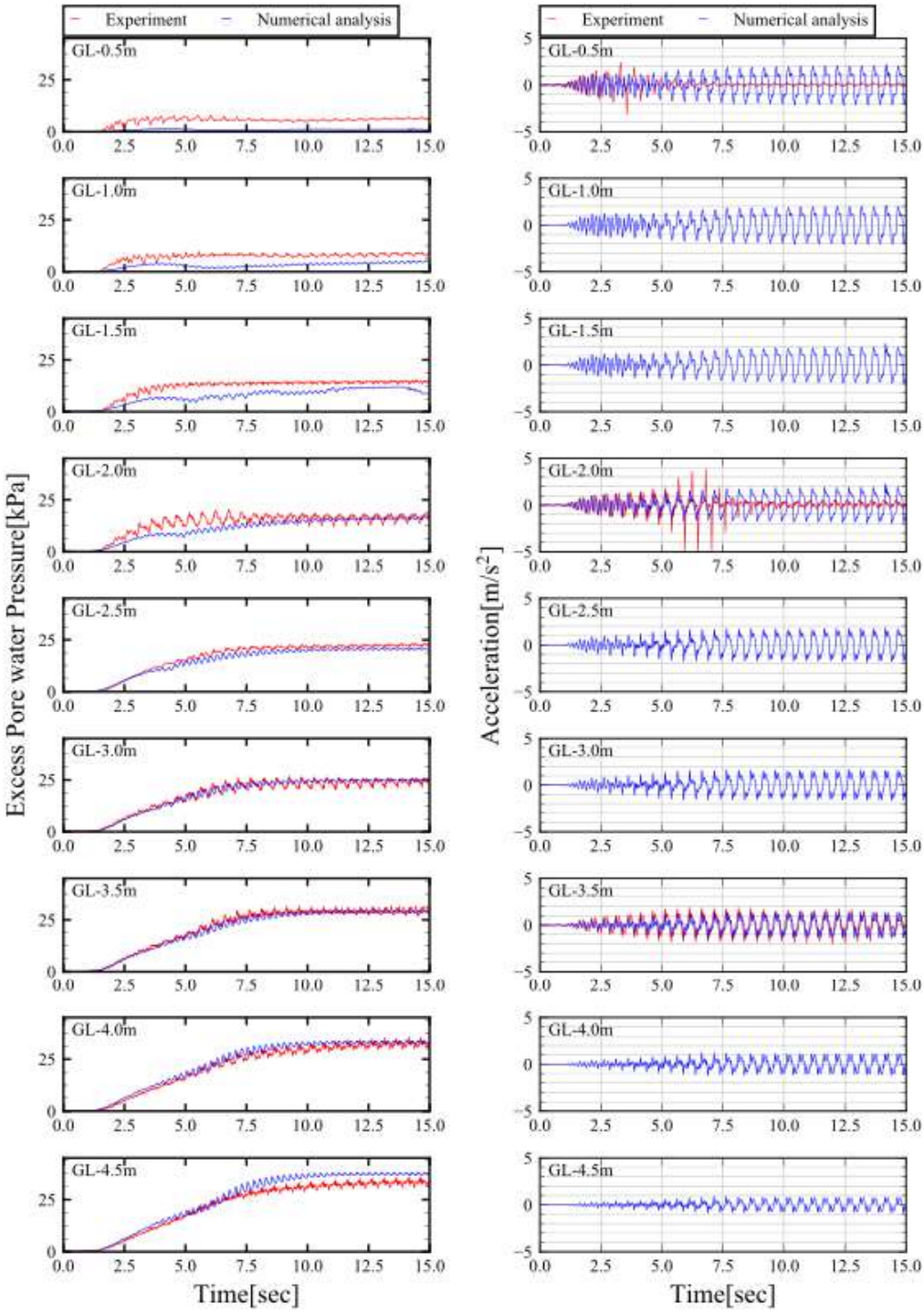

Figure 7. Comparison of the experimental and numerical result of the excess pore water pressure and acceleration.

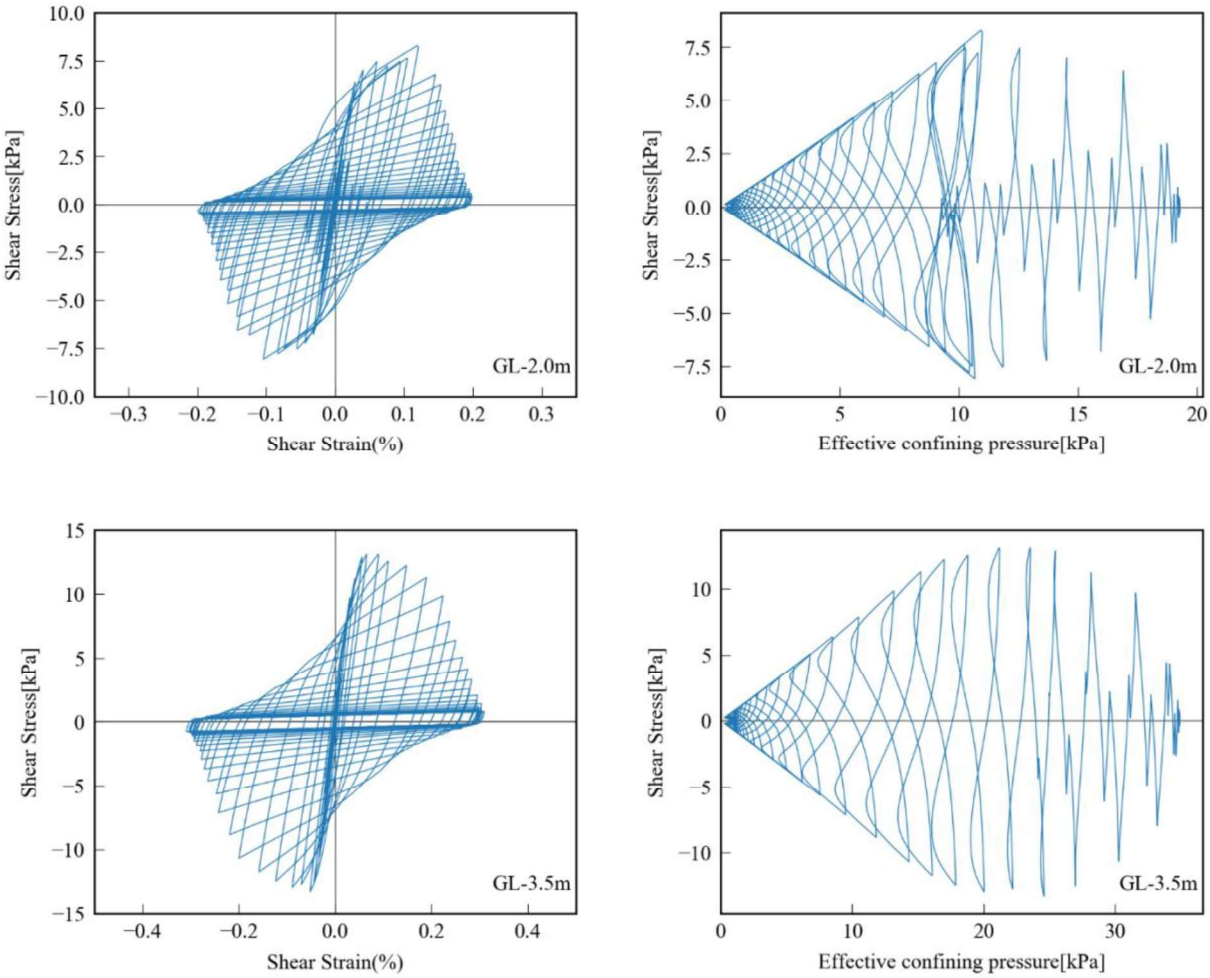

Figure 8. Proposed model results of shear strain and shear stress relationship and effective stress path.

7. References

[1] Fujisawa, K., Murakami, A., & Nishimura, S. I. (2010). Numerical analysis of the erosion and the transport of fine particles within soils leading to the piping phenomenon. *Soils and foundations*, **50**(4), 471-482.

[2] Nishimura, N. (1999). Chapter 3 Soil Mechanics, Geotechnical Engineering Handbook. *Japanese Geotechnical Society*, pp.51-64.

[3] Indraratna, B., Muttuvel, T. and Khabbaz, H. (2009): Modelling the erosion rate of chemically stabilized soil incorporating tensile force-deformation characteristics, *Canadian Geotechnical Journal*, **46**(1), 57–68.

[4] Uemura, K., 2010. Effects of soil sample disturbance on liquefaction induced strain development. Hiroshima University. *Master Thesis.* pp. 87 (in Japanese)

[5] Watanabe, A., Uzuoka, R., Ueda, K. (2018) Development of methods to evaluate the permeability of liquefied sand. Proc of The 53th Annual Meeting of the Japan National Conference on Geotechnical Engineering, No.948(E-08).

